

Supplementary Methods

Quantitative RT-PCR

Isolation of total RNA and analysis by RT-qPCR was conducted as described previously (1). Residual DNA was removed using the TURBO DNA-free kit (Thermo Fischer). For detection of mature miR-21 levels, TaqMan stem-loop qPCR was used (Thermo Fisher Scientific, Scoresby, Vic, Australia) as described previously (2). U6 snRNA was used as an internal reference gene (miRBase ID: 715680, Assay ID: 001973). For detection of protein-encoding mRNAs, single stranded cDNA was generated using ProtoScript II reverse transcriptase (New England Biolabs, Australia) and random pentadecamers.

Expression of mouse *Ecm1*, *Nes* and *Trip13* was determined using the SYBR Green real-time PCR master mix (Thermo Fischer) with ribosomal protein S27a (*Rps27a*) as an internal control. The oligonucleotide primer sequences used are as follows. *Ecm1_F*, 5' AAC CTG CCG CAG ACT GGC TA 3'; *Ecm1_R*, 5' GCA TCC TCC CAC ACA AGC TTC A 3'. *Nes_F*, 5' GCA GCA ACT GGC ACA CCT CAA 3'; *Nes_R*, 5' GCT TCA GCT TGG GGT CAG GAA A 3'. *Trip13_F*, 5' CCT GGA ACC GGG TGG TGC TG 3'; *Trip13_R*, 5' ATA CCG GTA CCT GCT CGA CAG TCT 3'. *Rps27a_F*, 5' CGG GGA AAA CCA TCA CGC TCG AGG TT 3'; *Rps27a_R*, CGG CCA TCT TCC AGC TGC TTA CCA GC 3'. PCR reactions were run for 45-50 cycles in 96-well Fast optical reaction plates using a StepOne-Plus or ViiA 7 real-time PCR system (Thermo Fisher).

Western blotting

Cells were lysed with cold lysis buffer (2% SDS and 50 mM Tris-HCl) and heated at 95 °C for 10 minutes. Large protein aggregates or genomic DNA were sheared by passing the lysates through a needle and syringe several times. Proteins were dissolved in 0.1 M DTT, 4% glycerol and 0.0004% bromophenol blue in lysis buffer) and subjected to gel electrophoresis and transferred to PVDF membranes (Millipore) using the Bolt system (Thermo Fisher). Membranes were blocked with 5% milk in PBS and incubated with primary antibodies (**Table S2**) at 4°C overnight. Following incubation with HRP-conjugated secondary antibodies, protein signals were detected using the enhanced chemiluminescence substrate (PerkinElmer). For assessment of multiple proteins on one membrane, immunostaining was done sequentially, knowing that each protein was located at a different molecular weight on the membrane. Antibodies used for each blot had been tested previously to demonstrate that each protein ran at a unique molecular weight. Images of the same blot were overlayed to ensure that bands produced by different antibodies did not overlap. When stripping was required to

reduce the intensity of previously stained bands, membranes were washed with warm stripping buffer (1.5% glycine, 0.1% SDS and 1% Tween 20, pH 2.2) four times for 5 minutes each time, followed by blocking and antibody detection.

RNA-Sequencing analysis

4T1.13-VC and 4T1.13-miR21KD orthotopic tumours (n = 4 per line) were recovered at day 14 as regression of 4T1.13-miR21KD tumours commenced. Total RNA was isolated using the Ambion miRVana total RNA isolation kit (Thermo Fisher). RNA was quantified using the Qubit RNA HS Assay Kit (Thermo Fisher) and 5 μ g treated with DNase I (Ambion Turbo DNA-free kit, Thermo Fisher). RNA-Seq was completed by the Australian Genome Research Facility (AGRF, Melbourne, Australia) on the Illumina HiSeq with 100bp SE sequencing using v4 chemistry, with 12 samples multiplexed in a single lane. Single-end 100bp reads were mapped to RefSeq mm10 genome build using subread (3). Read counts at the gene level were quantified using featureCounts (4). Gene counts with counts-per-million (cpm) larger than 0.5 in at least four samples were retained and normalized by TMM normalization (Robinson and Oshlack, 2010). Differential gene expression analysis was completed using the edgeR Quasi-likelihood Negative Binomial Generalized log-linear model framework (5). Genes with FDR<0.05 were determined as differentially expressed. Biological process-related gene ontology terms (annotated in the GO.db package) that are enriched in 4T1.13-miR21-KD tumours were identified using the *fry* function in the limma package.

Proteomic analysis

In gel digestion

Equal amounts of whole cell lysates were loaded onto precast NuPAGE® 4–12% Bis-Tris gels in 1x MES SDS running buffer. Gels were run at a constant voltage of 150 V followed by visualization of proteins with Coomassie stain (Bio-Rad). Gel bands (20) were excised and subjected to in-gel reduction, alkylation and trypsinization as described previously (6). Briefly, gel bands were reduced with 10 mM DTT (Bio-Rad), alkylated with 25 mM iodoacetamide (Sigma) and digested overnight at 37°C with 150 ng of sequencing grade trypsin (Promega). The tryptic peptides were extracted by 0.1% trifluoroacetic acid in 50% (w/v) acetonitrile.

LC-MS/MS

Samples were analysed by LC-MS/MS using Q-Exactive plus and Fusion Lumos Orbitrap mass spectrometers (Thermo Scientific), both fitted with nanoflow reversed-phase-HPLC (Ultimate 3000 RSLC, Dionex). The nano-HPLC system was equipped with an Acclaim Pepmap nano-

trap column (Dionex – C18, 100 Å, 75 µm × 2 cm) and an Acclaim Pepmap RSLC analytical column (Dionex – C18, 100 Å, 75 µm × 50 cm). Typically, for each LC-MS/MS experiment, 1µL of the peptide mix was loaded onto the enrichment (trap) column at an isocratic flow of 5µL/min of 3% CH₃CN containing 0.1% formic acid for 5 min before the enrichment column was switched in-line with the analytical column. The eluents used for the LC were 0.1% (v/v) formic acid (solvent A) and 100% CH₃CN/0.1% (v/v) formic acid (solvent B). The gradient used was 3% B to 25% B for 23 min, 25% B to 40% B in 2 min, 40% B to 85% B in 2 min and maintained at 85% B for 2 min before equilibration for 10 min at 3% B prior to the next injection. All spectra were acquired in positive mode with full scan MS spectra scanning from m/z 300–1650 in the FT mode at 70 000 (QE) and 120,000 (Lumos) resolution. Lockmass of 445.12003 m/z was used for both instruments. For MS/MS on the Lumos, the “top speed” acquisition method mode (3 sec cycle time) on the most intense precursor was used whereby peptide ions with charge states ≥2 were isolated with isolation window of 1.6 m/z and fragmented with HCD using normalized collision energy of 35. For MS/MS on the QE plus, the 15 most intense peptide ions with charge states ≥2 were isolated with isolation window of 1.6 m/z and fragmented by HCD with normalized collision energy of 35. Dynamic exclusion of 30s was applied.

Database searching, protein identification and label-free spectral counting

Peak lists were extracted from raw mass spectrometry into the Mascot Generic File Format (MGF) using MsConvert with peak picking. The MGF files were then searched using X! Tandem (Sledgehammer edition version 2013.09.01.1) against a NR protein database. Search parameters used were: fixed modification (carboamidomethylation of cysteine; +57 Da), variable modifications (oxidation of methionine; +16Da and N-terminal acetylation; +42 Da), two missed tryptic cleavages, 20 ppm peptide mass tolerance and 0.6Da fragment ion mass tolerance. Proteins were quantified using the Normalized Spectral Abundance Factor (NSAF) method (7, 8).

Immunohistochemistry

Fresh tumours were fixed in 4% paraformaldehyde at 4°C overnight, dehydrated and embedded in paraffin. Sections (4µm) were rehydrated and equilibrated in PBS-Tween 20 (PBS-T). Endogenous peroxidases were inactivated in 3% hydrogen peroxide for 10 min. Antigen retrieval was not required for anti-CD45, CD4 or CD8 antibodies. For rabbit cyclin D1, phospho-histone H3, cleaved caspase 3 and BAX antibodies, antigen retrieval was performed with citrate buffer (pH6) at sub-boiling temperature in a microwave for 12 minutes.

Information of the antibodies and their dilutions can be found in Supplementary Table 2. Sections were blocked with 3% normal goat serum in PBS-T at room temperature for 1h, followed by incubation with the primary antibodies in blocking buffer at 4°C overnight. Following incubation with biotin-conjugated goat anti-rat secondary antibodies (1:200 dilution) and the avidin-biotin complex (ABC) reagent (Vector Laboratories, Burlingame, CA, USA), sections were stained with 3,3' diaminobenzidine (DAB), counterstained with haematoxylin, and mounted in entellan.

Supplementary Data References

1. Johnstone CN, Smith YE, Cao Y, Burrows AD, Cross RS, Ling X, et al. Functional and molecular characterisation of EO771.LMB tumours, a new C57BL/6-mouse-derived model of spontaneously metastatic mammary cancer. *Dis Model Mech.* 2015;8(3):237-51.
2. Kong W, Yang H, He L, Zhao JJ, Coppola D, Dalton WS, et al. MicroRNA-155 is regulated by the transforming growth factor beta/Smad pathway and contributes to epithelial cell plasticity by targeting RhoA. *Molecular and cellular biology.* 2008;28(22):6773-84.
3. Liao Y, Smyth GK, Shi W. The Subread aligner: fast, accurate and scalable read mapping by seed-and-vote. *Nucleic Acids Res.* 2013;41(10):e108.
4. Liao Y, Smyth GK, Shi W. featureCounts: an efficient general purpose program for assigning sequence reads to genomic features. *Bioinformatics.* 2014;30(7):923-30.
5. Robinson MD, Oshlack A. A scaling normalization method for differential expression analysis of RNA-seq data. *Genome Biol.* 2010;11(3):R25.
6. Mathivanan S, Ji H, Tauro BJ, Chen YS, Simpson RJ. Identifying mutated proteins secreted by colon cancer cell lines using mass spectrometry. *J Proteomics.* 2012;76 Spec No.:141-9.
7. Samuel M, Fonseka P, Sanwlani R, Gangoda L, Chee SH, Keerthikumar S, et al. Oral administration of bovine milk-derived extracellular vesicles induces senescence in the primary tumor but accelerates cancer metastasis. *Nat Commun.* 2021;12(1):3950.
8. Paoletti AC, Parmely TJ, Tomomori-Sato C, Sato S, Zhu D, Conaway RC, et al. Quantitative proteomic analysis of distinct mammalian Mediator complexes using normalized spectral abundance factors. *Proc Natl Acad Sci U S A.* 2006;103(50):18928-33.

Supplementary Table Legends

Supplementary Table 1

Gene Ontology (GO) analysis of the transcriptomes of primary tumours derived from 4T1.13-VC and 4T1.13-miR-21-KD tumours.

Supplementary Table 2

Source of antibodies used in this study.

Supplementary Table 3

Proteins detected by mass spectrometry in three biological replicates of 4T1.13-miR-21-KD (4TM), 4T1.12-VC (4TV), EO771.LMB-miR-21 (EOM) and EO771.LMB-VC (EOV).

Supplementary Table Legends

Supplementary Table 1

Gene Ontology (GO) analysis of the transcriptomes of primary tumours derived from 4T1.13-VC and 4T1.13-miR-21-KD tumours.

Supplementary Table 2

Source of antibodies used in this study.

Supplementary Table 3

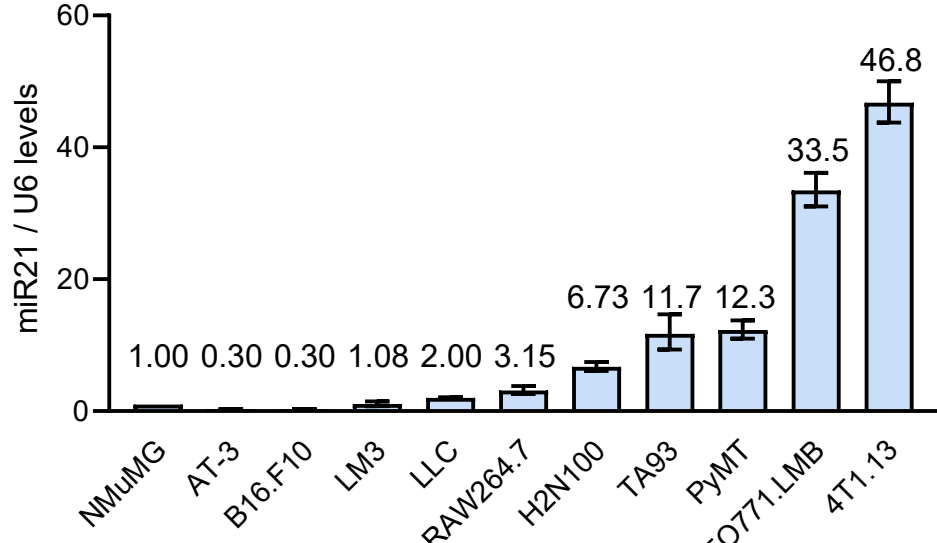
Proteins detected by mass spectrometry in three biological replicates of 4T1.13-miR-21-KD (4TM), 4T1.12-VC (4TV), EO771.LMB-miR-21 (EOM) and EO771.LMB-VC (EOV).

Supplementary Table 2. List of antibodies used in western blotting, immunohistochemistry, and flow cytometry. All flow cytometry antibodies were rat anti-mouse.

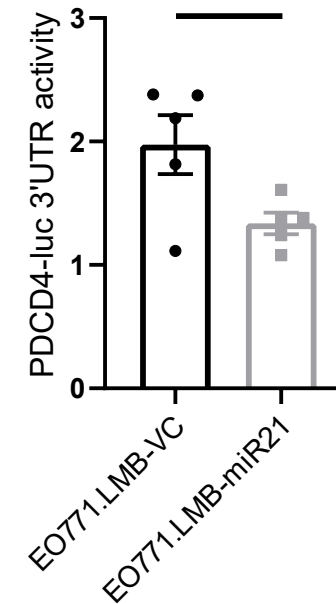
Target	Clone(s)	Fluorochrome	Dilution	Source
PD_CD4	D29C6	N/A: For western	1:1,000	CST
PTEN	D4.3	N/A: For western	1:1,000	CST
HSP90	EPR16621-67	N/A: For western	1:1,000	Abcam
CD45	30-F11	N/A: For IHC	1:200	BD Pharmingen
Cyclin D1	E3P5S	NA: For western and IHC	WB: 1:1,500 IHC: 1:500	CST
Phospho-histone H3 (S10)	Cat#9701	NA: For western and IHC	WB: 1:1,500 IHC: 1:500	CST
Cleaved caspase 3 (D175)	Cat#9661	NA: For western and IHC	WB: 1:1,500 IHC: 1:500	CST
BAX	Cat#554106	NA: For western and IHC	WB: 1:1,500 IHC: 1:500	BD Pharmingen
CD4	4SM95	N/A: For IHC	1:200	Invitrogen
CD8α	4SM15	N/A: For IHC	1:200	eBioscience/Affymetrix
CD16/CD32	2.4G2	N/A	1:300	BD Biosciences
CD45.2	104	APC	1:300	eBioscience/Invitrogen
TCRβ	H57-597	PE-Cy7	1:200	BD Biosciences
CD8α	53-6.7	APC-Cy7	1:400	BD Biosciences
CD4	RM4.5	PE-Cy5	1:500	BD Biosciences
CD69	H1.2F3	PE	1:100	eBioscience/Invitrogen
CD49b	Dx5	BV421	1:100	BD Biosciences
CD11b	M1/70	APC-Cy7	1:1,000	BD Biosciences
Ly6C	AL-21	BV421	1:500	BD Biosciences
Ly6G	1A8	PE-Cy7	1:1,000	BD Biosciences
CD206	C068C2	BV711	1:200	BioLegend
PD-L1	MIH5	PE	1:200	eBioscience/Invitrogen
CD11c	HL3	BV510	1:100	BD Biosciences
MHC class II	M5/114.15.2	PE	1:400	eBioscience/Invitrogen
NKp46	29A1.4	BV510	1:100	BD Biosciences

Figure S1

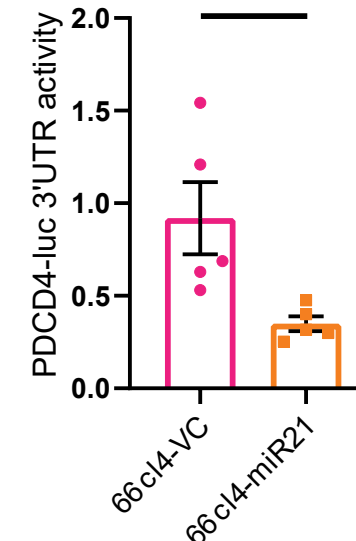
a



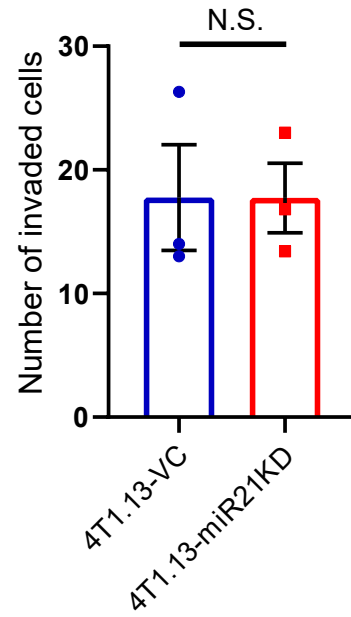
b (i)



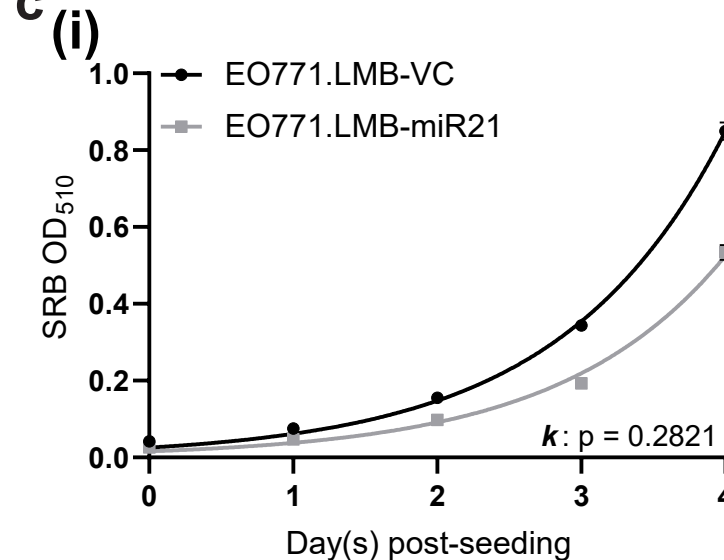
(ii)



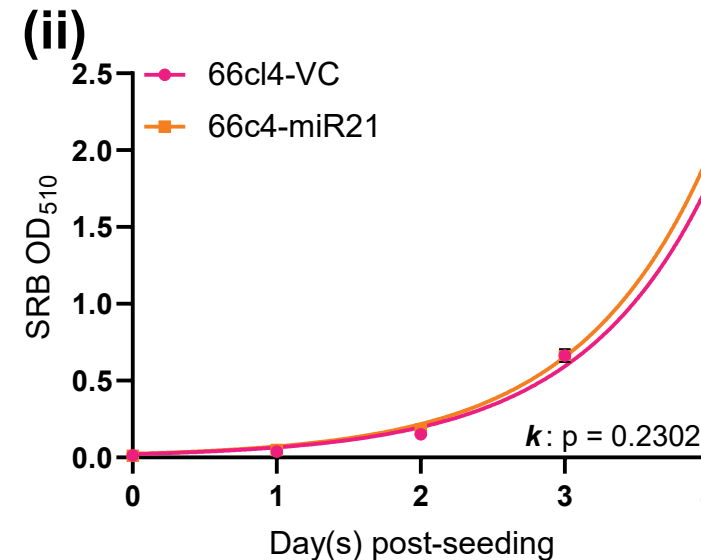
d



c



(i)



(ii)

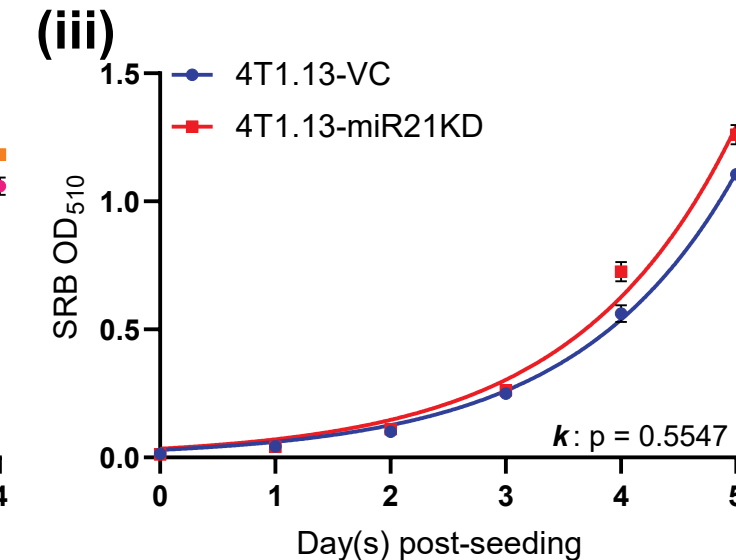


Figure S1. Effect of miR-21 on mouse mammary cancer cells *in vitro*.

(a) MiR-21 expression levels in a panel of normal or transformed mouse cell lines. Mean +/- SEM (n=3). Expression in NMuMG immortalised mouse mammary epithelial cells was set to 1. **(b)** Validation of miR-21 overexpression in EO771.LMB (i) and 66cl4 (ii) cells as measured by PDCD4 3'UTR reporter gene activity. Mean +/- SEM (n=5). **(c)** Effect of modulation of miR-21 levels or activity on the proliferative capacity of EO771.LMB (i), 66cl4 (ii) and 4T1.13 cells (iii). Mean +/- SEM (n=6). Statistical analysis of the proliferation rate parameter (k) was performed by the exponential growth equation function in Prism. **(d)** Effect of loss of miR-21 activity on the invasive capacity of 4T1.13 cells. Mean +/- SEM (n=3).

Figure S2

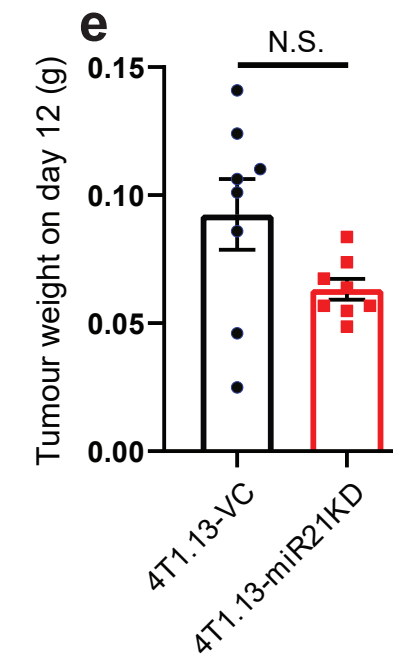
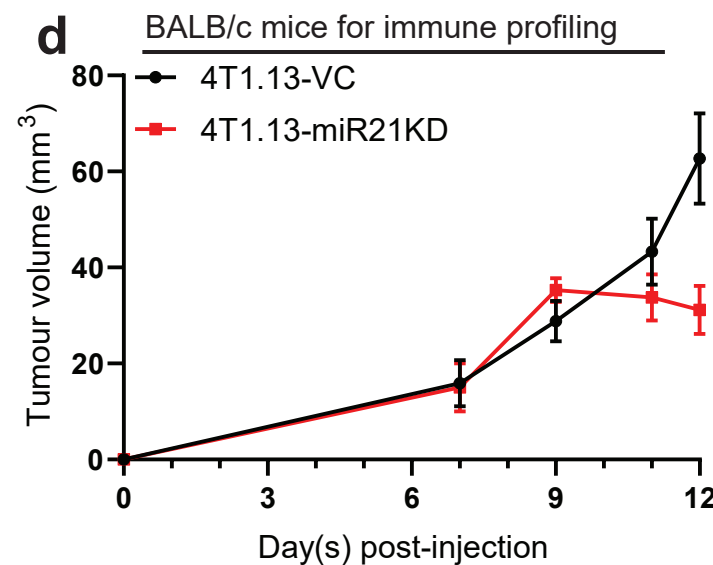
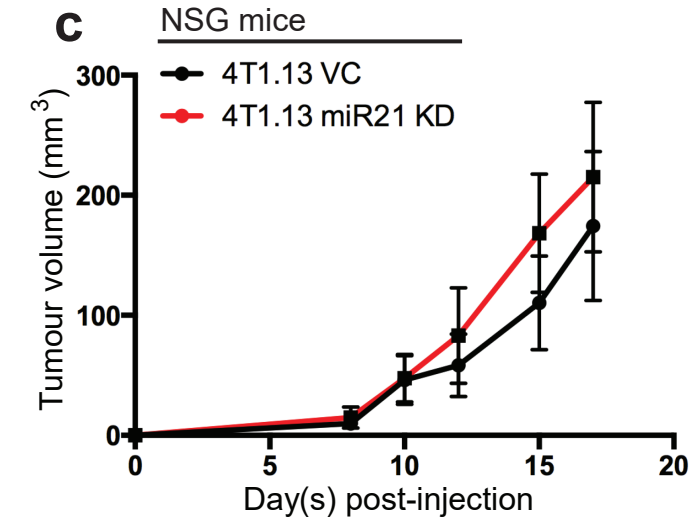
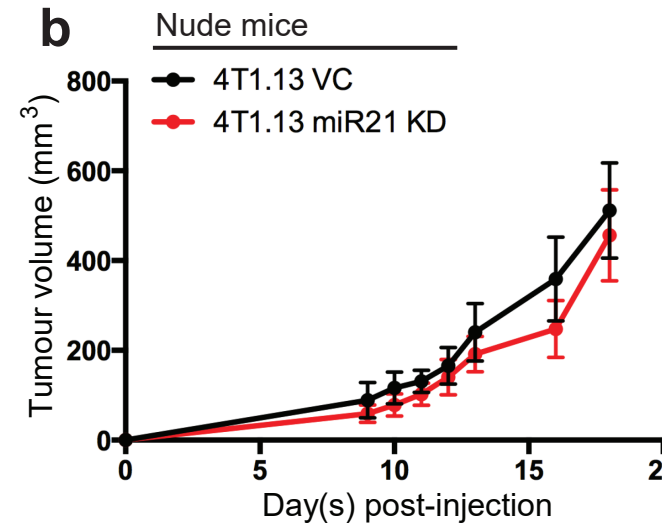
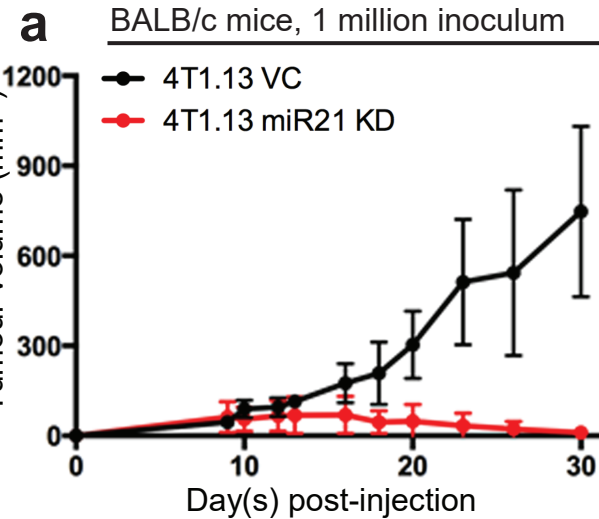


Figure S2. Effect of miR-21 on mammary tumour growth.

a) Effect of loss of miR-21 activity on the growth rate of 4T1.13 mammary tumours, following an increased inoculum of 1×10^6 cells (n=13). **(b-c)** Effect of loss of miR-21 activity on the growth rate of 4T1.13 tumours in Balb/c nu/nu **(b)** or NSG **(c)** mice following an inoculum of 2×10^5 cells (n=10). **(d-e)** Growth kinetics and weights of 4T1.13 tumours on day 12 in BALB/c mice used for immune profiling in Figure 4. Displayed as mean+/-SEM.

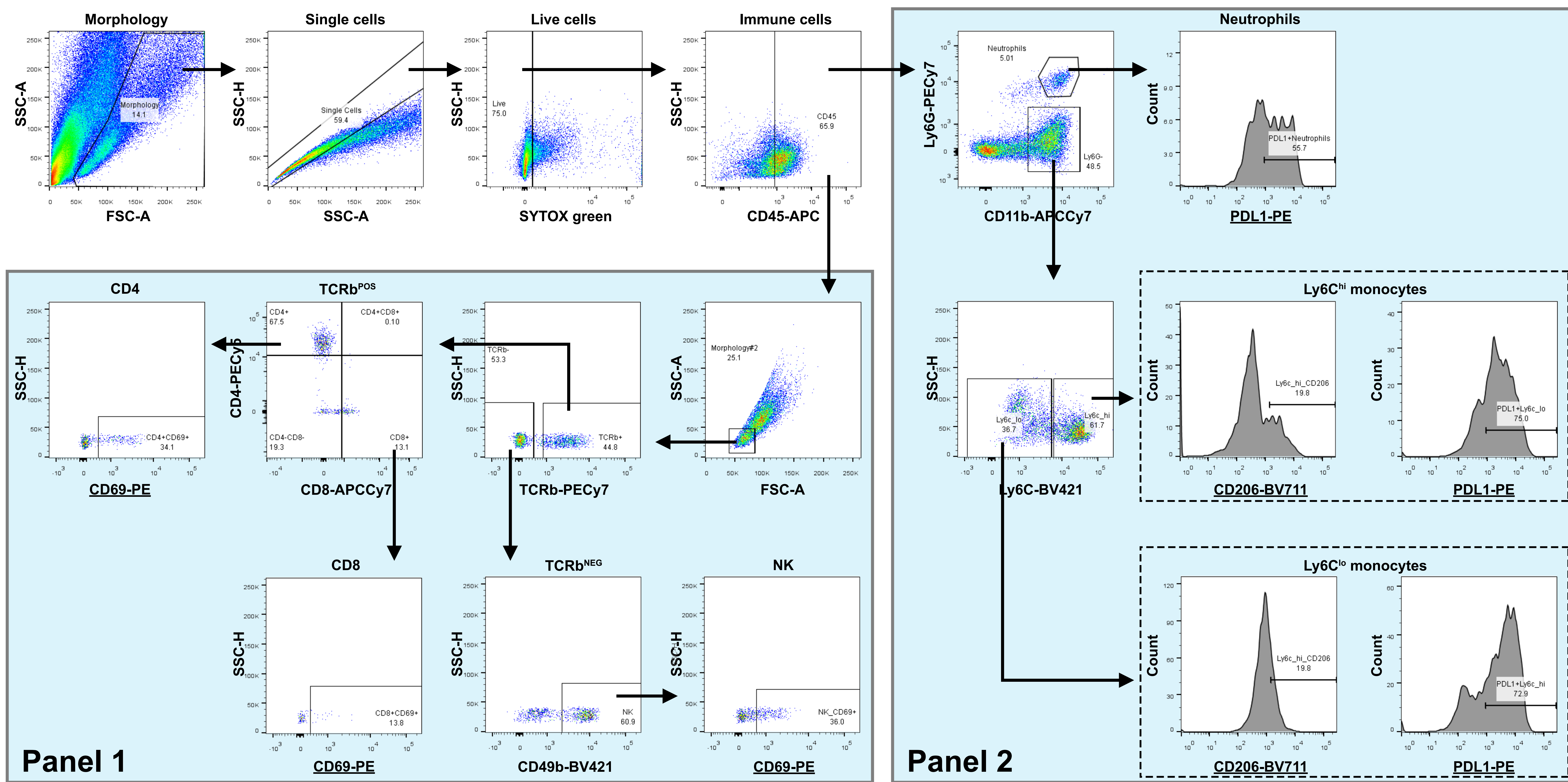
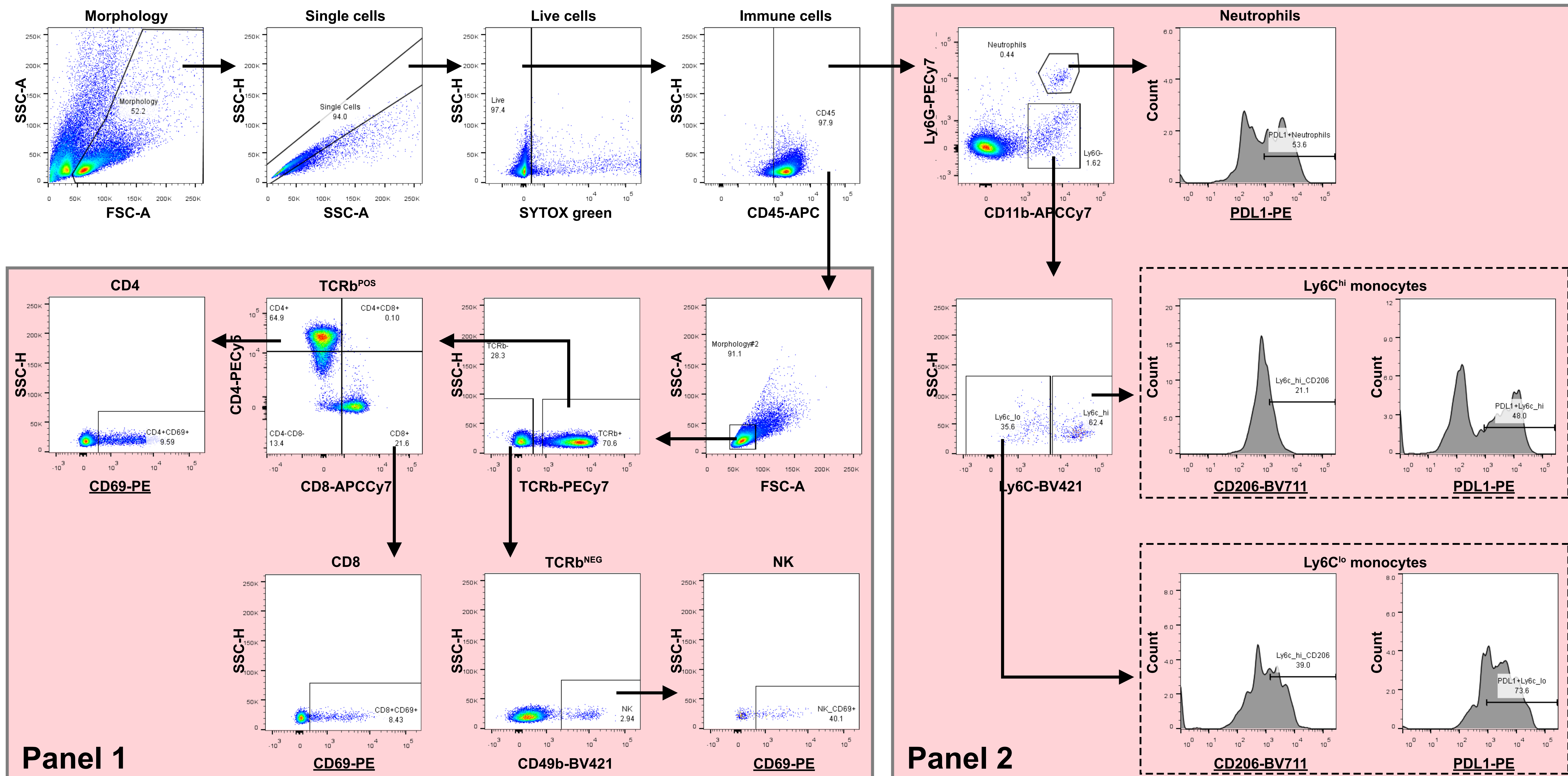
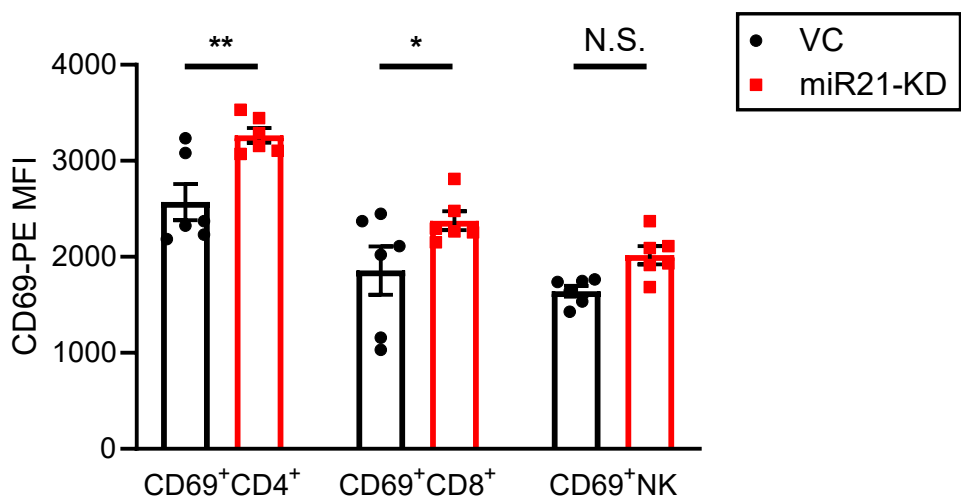
a**4T1.13-VC****b****4T1.13-miR21KD**

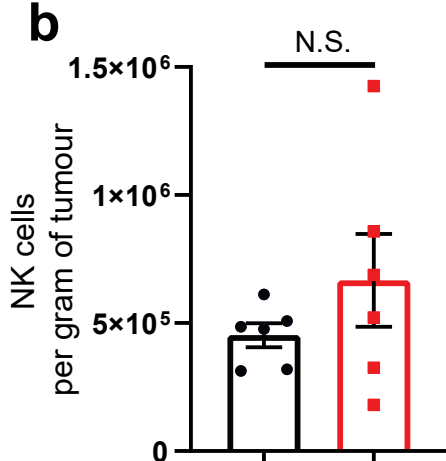
Figure S3. Gating strategies for lymphocytes and myeloid cells in 4T1.13 tumours. The antibodies used are listed in **Table S2**. Gating for underlined antibodies was based on the fluorescence minus one (FMO) controls.

Figure S4

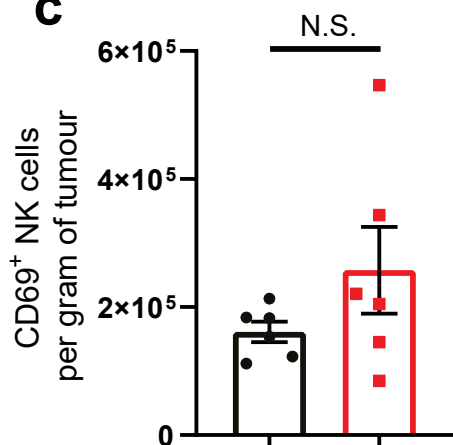
a



b



c



d

KEGG_NATURAL_KILLER_CELL_MEDIATED_CYTOTOXICITY

PValue = 0.004 ; PValue Mixed = 0.002

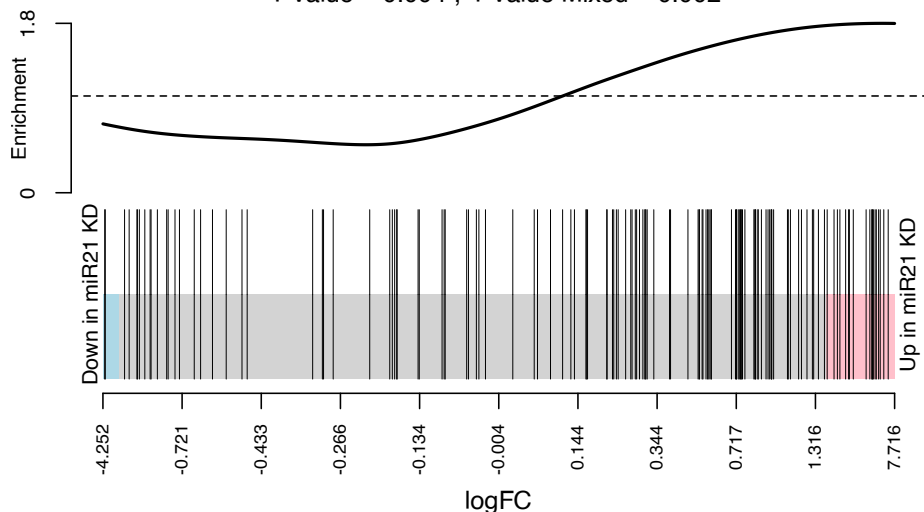
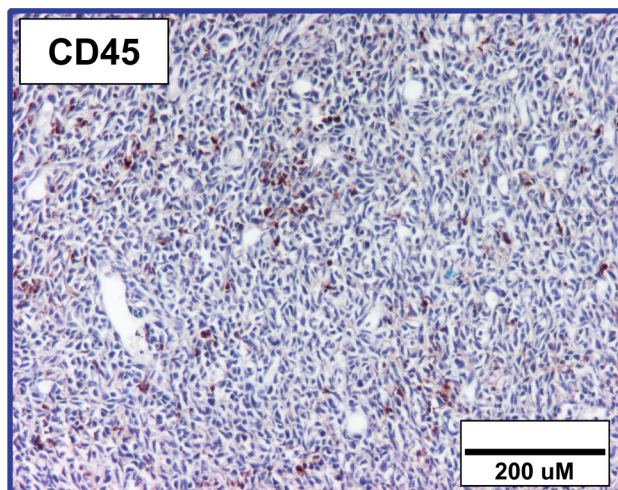


Figure S4. Immune profiling of 4T1.13 tumours

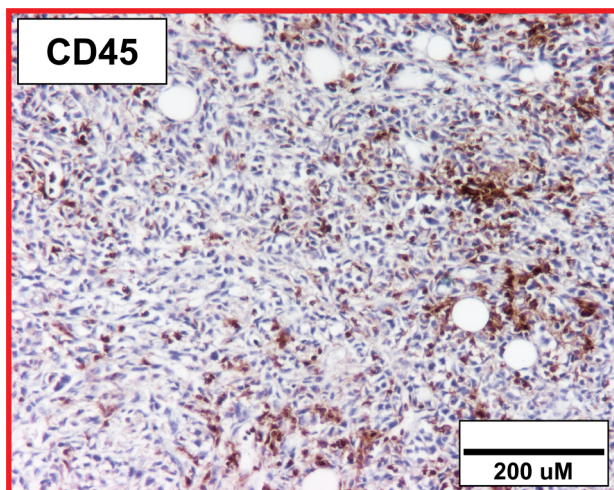
(a) Mean fluorescence intensity (MFI) of CD69 on CD4⁺ and CD8⁺T cells and on NK cells infiltrating 4T1.13-VC and 4T1.13-miR-21-KD tumours. **(b-c)** Effect of loss of miR-21 activity on the number of NK cells (b) or CD69⁺NK cells (c) infiltrating 4T1.13-VC and 4T1.13-miR-21-KD tumours. **(d)** Barcode plot of enrichment of NK cell mediated cytotoxicity in the 4T1.13-miR-21-KD tumours.

Figure S5

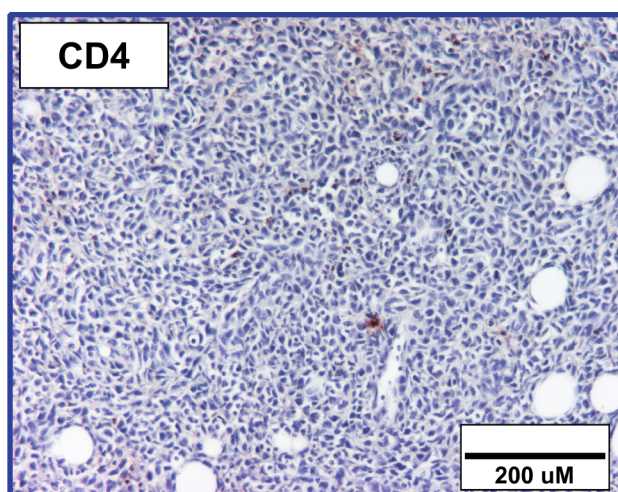
4T1.13-VC



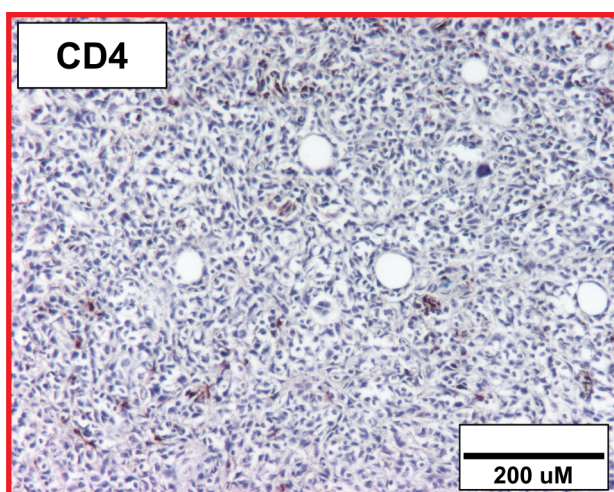
4T1.13-miR21KD



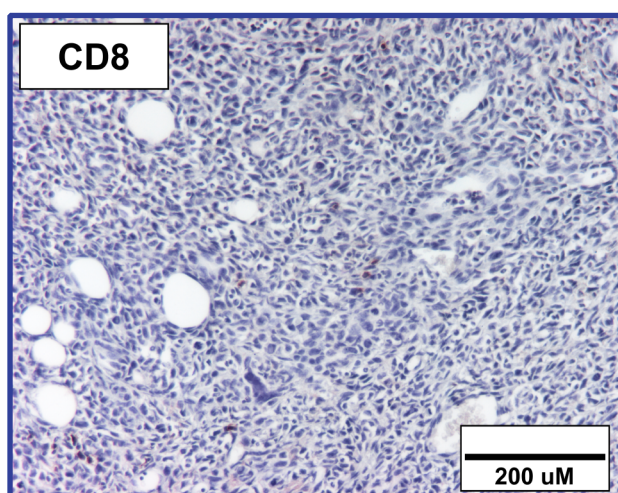
CD4



CD4



CD8



CD8

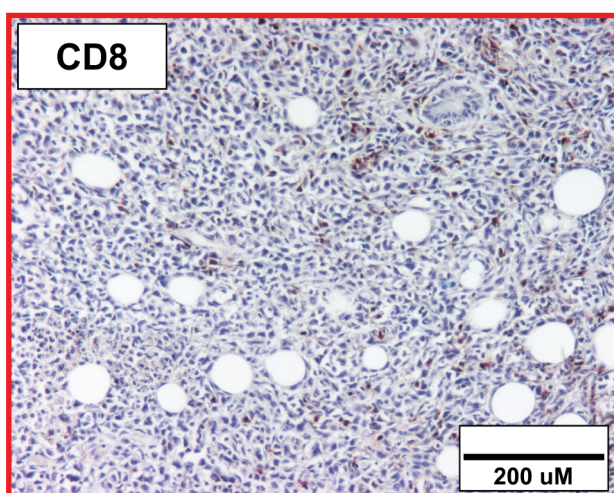


Figure S5. Immunohistochemical validation of T cells.

Changes in CD45⁺ total immune cell infiltrates, in CD4⁺ and CD8⁺T cell infiltrates in 4T1.13-miR-21-KD compared to 4T1.13-VC tumours as assessed by immunohistochemistry (VC: EO771.LMB-VC; OE: EO771.LMB-miR-21).

Figure S6

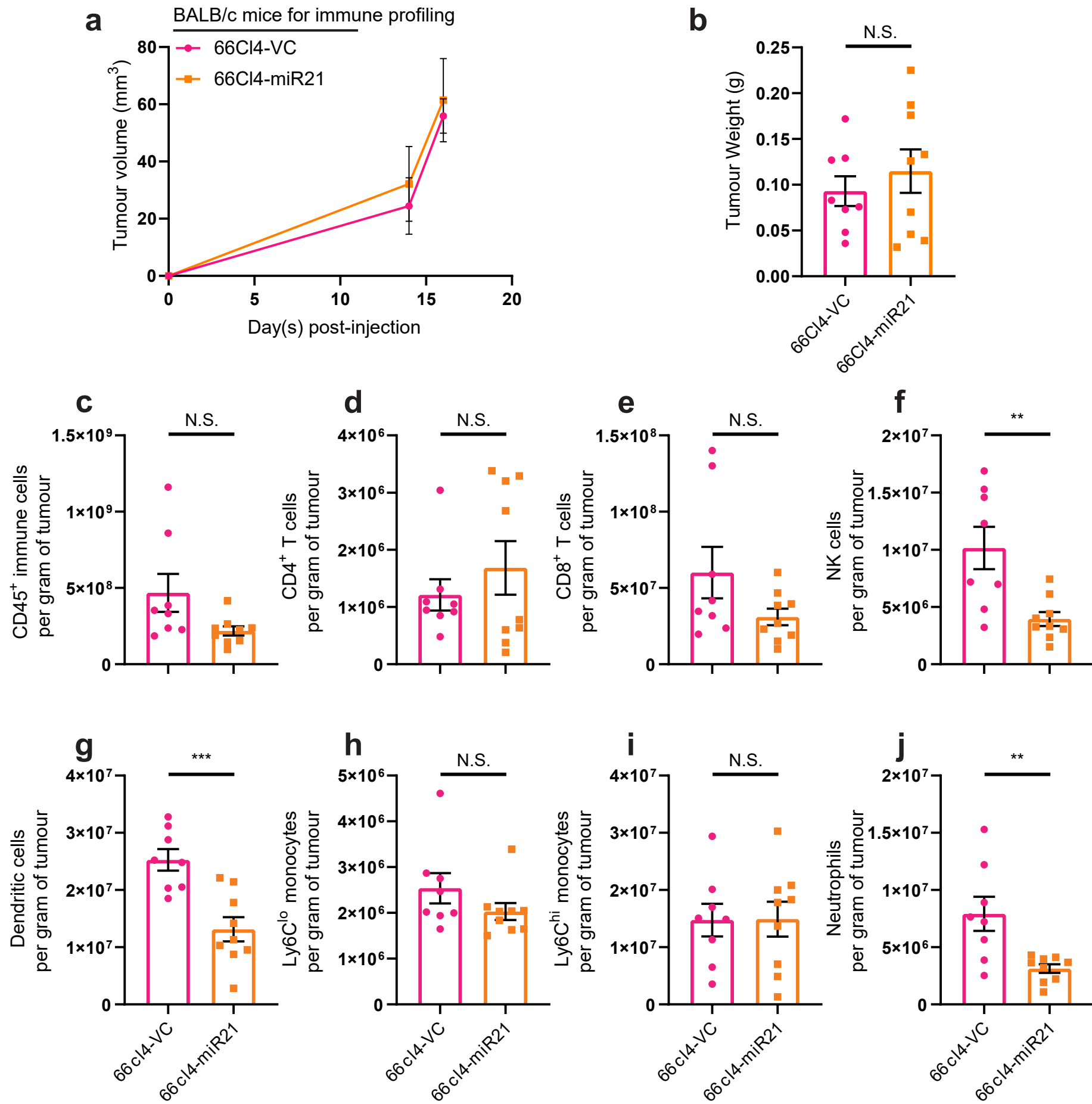


Figure S6. Immune profiling of 66cl4 tumours with miR-21 overexpression.

(a-b) Growth kinetics and weights of 66cl4 tumours used for immune profiling. Cells (5×10^5) were injected into the mammary gland of BALB/c mice and removed on day 17 for immune cell profiling. Mean +/- SEM (n=8 for the 66cl4-VC group, and n=9 for the 66cl4-miR-21 group). **(c-j)** Total numbers of immune infiltrates per gram of tumour in the 66cl4-VC and 66cl4-miR-21 groups. Mean +/- SEM (n=8 for the 66cl4-VC group, and n=9 for the 66cl4-miR-21 group).

Figure S7

EO771.LMB

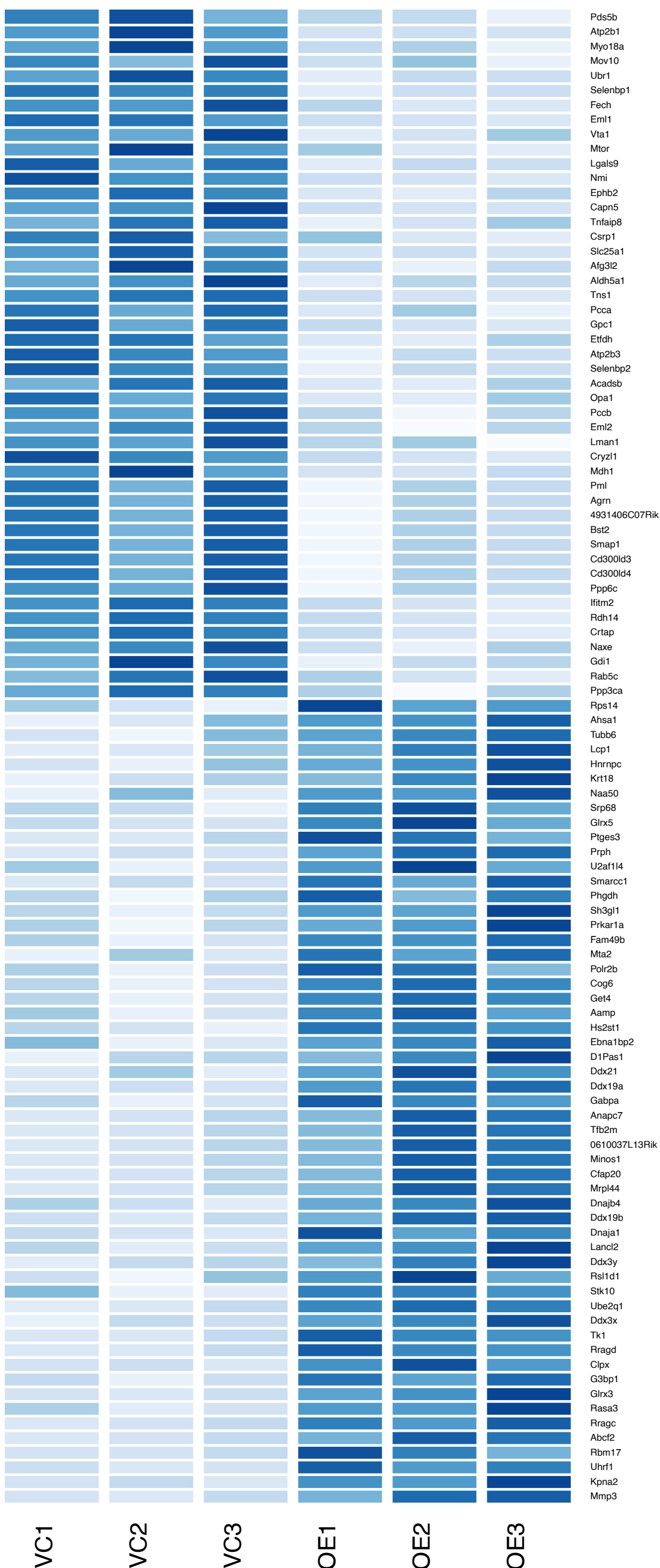
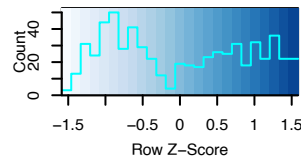


Figure S7. Proteomic analysis of EO771.LMB-VC and EO771.LMB-miR-21 cells,
showing the top differentially expressed proteins in triplicate samples of the two cell lines.